DOI 10.1007/s10778-018-0920-0
*International Applied Mechanics, Vol. 54, No. 6, November, 2018*

# MODELING THE DEFORMATION OF ORTHOTROPIC TOROIDAL SHELLS WITH ELLIPTICAL CROSS-SECTION BASED ON MIXED FUNCTIONALS

**I. V. Lutskaya*, V. A. Maximuk*, and I. S. Chernyshenko****

**Static problems for toroidal shells with elliptical cross-section made of elastic orthotropic composites are considered. Variational difference and Lagrange multiplayer methods with mixed functionals are used. The ellipticity of the cross-section is significant. Emphasis is placed on the accuracy of the results. The agreement between the internal and external forces in the transverse and longitudinal sections is used as an integral criterion.**

**Keywords:** shell theory, Lagrange multipliers, toroidal composite shell, significant ellipticity, locking effect

**Introduction.** The classical application of toroidal shells due to more compact arrangement compared with cylinders is high-pressure vessels [5]. The efforts to optimize structures resulted in toroidal shells of noncircular cross-sections [6, 20], including elliptical cross-sections [4, 16, 17, 19], and shells of variable thickness and reinforced shells [17].

Of certain interest are closed toroidal shells as elements of space structures, including superlight inflatable satellite components such as antenna elements that support space telescopes [11, 12, 13, 18]. Inflatable toroidal membranes are also used in biomechanics, medicine, and other fields [12]. Of special interest are open thin-walled toroidal shells [12].

Toroidal shells are of theoretical interest in testing shell design methods because at certain ratios among the parameters of such shells, they take the shape of structures whose stress–strain state (SSS) in certain parts is obvious [4]. Moreover, such shells can also be used for testing so-called membrane locking [10]. It should be noted that such tests are mainly two-dimensional. The axisymmetrical deformation of shells of revolution with double curvature occurs without membrane locking owing to self-reinforcement. However, membrane locking can be observed in a closed toroidal shell with elliptical cross-section under internal pressure [4]. In this case, the cross-section, as in a long cylindrical shell, tends to take a circular shape, which under moderate tension results in significant bends near the major and minor half-axes [2, 14, 15]. Therefore, using numerical methods without measures taken to prevent locking may worsen the convergence [4].

To improve the convergence, mixed functionals with additional variation of small strain components can be used [4]. This approach is universal. To avoid the membrane locking, it is possible to construct a mixed functional with additional variation of membrane strains.

In what follows, we will discuss the results of numerical analysis of the axisymmetric SSS of thin-walled toroidal shells of elliptical cross-section made of orthotropic composite materials. We will employ the variational-difference method (VDM) with mixed functionals. The basic relations and governing equations of the theory of deep orthotropic shells and a technique for solving boundary-value problems are outlined in [1, 10]. The convergence of the method was been analyzed in [4] depending on the number of varied functions.

**1. Problem Statement.** Let us consider a closed toroidal shell of revolution with elliptical cross-section (Fig. 1). Assume that the shell mid-surface is generated by revolving an ellipse around the $Oz$-axis in a Cartesian coordinate system $(x, y, z)$. The ellipse is described by

S. P. Timoshenko Institute of Mechanics, National Academy of Sciences of Ukraine, 3 Nesterov St., Kyiv 03057, Ukraine; e-mail: *desc@inmech.kiev.ua, **prikl@inmech.kiev.ua. Translated from Prikladnaya Mekhanika, Vol. 54, No. 6, pp. 57–62, November–December, 2018. Original article submitted September 26, 2017.

 

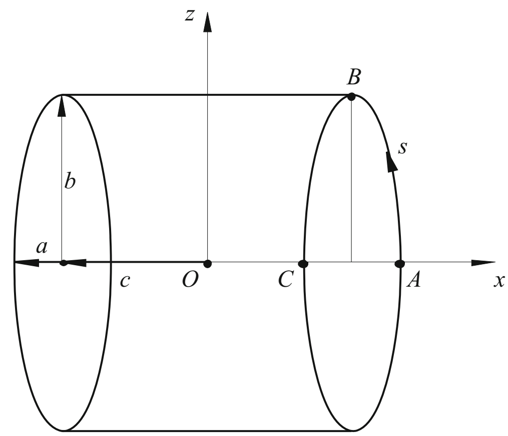


Fig. 1

$$F(x,z)=\left(\frac{x-c}{a}\right)^2+\left(\frac{z}{b}\right)^2-1=0, \tag{1}$$

where $a$ and $b$ are its half-axes, $c$ is the distance of the cross-sectional center from the axis of revolution [4].

Let the mid-surface be referred to a curvilinear coordinate system $(s,\theta,\gamma)$, where $\gamma$ is the normal coordinate, $s$ is the length of the elliptical arc reckoned counterclockwise from the point $A$ $(x=c+a,\ z=0)$ to the point $C$ $(x=c-a,\ z=0)$. The orthotropy axes of the material are aligned with the coordinate lines.

Assume that the SSS of the shells is described by the kinematical equations of the general theory of thin shells and the constitutive equations of elasticity of anisotropic media [1], while the governing equations are derived using the VDM. To simplify the implementation of the Kirchhoff–Love hypotheses, we will use mixed functional with undetermined Lagrange multipliers [10] representing shearing forces. Moreover, some strain components can additionally be varied.

The SSS of the shell under uniformly distributed internal pressure is axisymmetrical.

**2. Methodical Features of Problem Solving.** The original algorithm of numerical discretization of a plane curve [4] can be used to reduce Eq. (1) to parametrical form:

$$x=x(s), \qquad z=z(s).$$

The coefficients of the first quadratic form are determined as

$$A_s=1, \qquad A_\vartheta=r, \tag{2}$$

while the curvatures are calculated as follows [1]:

$$k_s=r'z''-r''z', \qquad k_\theta=z'/r, \tag{3}$$

where $r$ is the parallel radius, the "stroke" denotes differentiation with respect to $s$ performed numerically by difference formulas.

When the SSS of thin toroidal shells was analyzed in [4, 8] without measures against locking, the following mixed functional was used:

$$\Pi_1(u,w,\varphi_s,T_{s\gamma}^f)=\iint_\Omega A(u,w,\varphi_s)d\Omega-A_n-A_k+\iint_\Omega T_{s\gamma}^f\varepsilon_{s\gamma}d\Omega, \tag{4}$$

where $u$ and $w$ are the components of the displacement vector along the axes $(s,\gamma)$, respectively, $A$ is the strain energy density, $A_n$ and $A_k$ the works done by the surface and boundary forces, respectively. The geometrical part of the Kirchhoff–Love hypotheses in (4)

$$\varepsilon_{s\gamma}=0 \tag{5}$$

TABLE 1

| $\tilde{s}$ | $\tilde{\gamma}$ | $\sigma_s$, MPa | $\sigma_\theta$, MPa |
|---|---|---|---|
| 0 | 0.5 | 86.1 | 297.4 |
| | –0.5 | 86.1 | 297.4 |
| 0.5 | 0.5 | –184.5 | 107.6 |
| | 0 | 18.3 | 117.6 |
| | –0.5 | 221.1 | 127.5 |
| 1.0 | 0.5 | 141.7 | –98.6 |
| | –0.5 | 141.7 | –98.6 |

is implemented using the method of undetermined Lagrange multipliers $T_{s\gamma}^f$ representing shearing forces. The angle $\varphi_s$ of the normal is determined from (5) by varying (4).

To increase the convergence rate, we use mixed functional in which the membrane strain $\varepsilon_s^f$ is varied additionally. After eliminating the appropriate Lagrange multiplier, we arrive at the following functional [10]:

$$\Pi_2(u, w, \varphi_s, T_{s\gamma}^f, \varepsilon_s^f) = \Pi_1(u, w, \varphi_s, T_{s\gamma}^f) - \frac{1}{2}\iint_\Omega G_s(\varepsilon_s - \varepsilon_s^f)^2 \, d\Omega, \tag{6}$$

where $\varepsilon_s$ is a formula for the membrane strain $\varepsilon_s^f$, $G_s = E_s / (1 - \nu_s \nu_\theta)$, $E_s, \nu_s, \nu_\theta$ are elastic constants.

In the section $z = 0$, the following symmetry conditions are prescribed:

$$u = 0, \quad \varphi_s = 0, \quad T_{s\gamma}^f = 0. \tag{7}$$

Note that the third condition in (7), which is imposed on the shearing force, follows from the method of constructing functionals (4) and (6) because this force appears as an equivalent independent function together with the displacements and angle [8, 10]. However, the function $\varepsilon_s^f$ in (6) is not such due to the elimination of the Lagrange multiplier.

Varying (4) and (6), we arrive at a system of linear algebraic equations with symmetric band matrix [10].

**3. Analysis of the Numerical Results.** Let us analyze the SSS of a toroidal shell with the following geometrical parameters [4]: $\tilde{a} = a/h = 100$, $\tilde{b} = b/h = 1000$, $\tilde{c} = c/h = 200$, $\tilde{s} = s/s_k$ $= 2032$ is half the ellipse arc, $h$ is the shell thickness. As is seen, the shell cross-section is highly extended along the symmetry axis. The shell consists of two coaxial cylindrical shells joined at the ends and having different stresses and is made of glass-reinforced composite fabric with the following characteristics [1]: $E_s = 15$ GPa, $E_\theta = 12$ GPa, $\nu_s = 0.12$. It is subject to uniformly distributed internal pressure of intensity $q = 1$ MPa.

The half the elliptical arc was partitioned into a number of equally spaced nodal points ($K = 161\ldots 20481$) using the above algorithm [4] of numerical discretization of plane curve (1). The number of the nodal points was doubled until the maximum SSS components coincide in three significant digits. Moreover, we used two integral accuracy criteria: equality of the internal ($F$) and external ($P$) forces in the sections of the torus by the planes $Oxz$ and $z = 0$. In the first (vertical) section, they are calculated by

TABLE 2

| $K$ | $w_A$ | $w_B$ | $\sigma^+$, MPa | $\sigma^-$, MPa | $\widetilde{F}_\theta \cdot 10^{-5}$ | $\widetilde{F}_s \cdot 10^{-4}$ |
|---|---|---|---|---|---|---|
| 161 | 0.737 | –0.121 | 70 | 158 | 1.5039 | 10.8630 |
| 321 | 0.740 | –0.242 | 391 | –66 | 1.5880 | 3.0812 |
| 641 | 0.715 | 0.325 | –789 | 680 | 1.5806 | 33.8035 |
| 1281 | 0.722 | 0.199 | –364 | 407 | 1.5769 | 25.9413 |
| 2561 | 0.722 | 0.209 | –249 | 296 | 1.5736 | 25.2024 |
| 5121 | 0.724 | 0.222 | –203 | 243 | 1.5719 | 25.1321 |
| 10241 | 0.723 | 0.227 | –189 | 226 | 1.5712 | 25.1346 |
| 20481 | 0.723 | 0.228 | –185 | 221 | 1.5710 | 25.1327 |

$$F_\theta = h \int_0^{s_k} \sigma_\theta^0 ds, \qquad P_\theta = \frac{1}{2} \pi abq, \tag{8}$$

while in the second (horizontal) section by

$$F_s = 2\pi h[(c+a)\sigma_s^0(0) + (c-a)\sigma_s^0(s_k)], \qquad P_s = 4\pi acq, \tag{9}$$

where $\sigma_\theta^0$ and $\sigma_s^0$ are the hoop and meridional stresses in the shell mid-surface, respectively.

In [4], half the elliptic arc has to be divided by 20481 nodal points to achieve the same accuracy with the VDM using the functional $\Pi_1(u, w, \varphi_s, T_{s\gamma}^f)$, i.e., without taking special measures to prevent locking. Convergence was slow yet stable. The convergence was more rapid (Fig. 1) at the points $A$ $(s = 0)$ and $C$ $(s = s_k)$, where the stress state is nearly membrane (Table 1). The values of meridional $(\sigma_s)$ and hoop $(\sigma_\theta)$ stresses are given at typical points of the elliptical cross-section (values of $\widetilde{s} = s / s_k = 0$, 0.5, 1.0 correspond to the points $A$, $B$, $C$) and two or three points across the shell thickness $(\widetilde{\gamma} = \gamma / h = 0, \pm 0.5)$.

The convergence is especially slow (Table 2) near the major half-axis of the ellipse (point $B$, $\widetilde{s} = 0.5$), where the moment stresses are significant due to the large cross-sectional bending (unbending). Table 2 summarizes, depending on the number $K$ of points, the deflection $w_A = w(0)/h$ at the point $A$, the deflection $w_B = w(s_k)/h$, the stresses $\sigma^+$ and $\sigma^-$ on the outside and inside surfaces of the shell at the point $B$, and the dimensionless forces $\widetilde{F}_\theta = F_\theta / qh^2$ and $\widetilde{F}_s = F_s / qh^2$ in vertical and horizontal sections.

As can be seen, the internal forces converge with increasing number of partition points to their exact values $\widetilde{P}_\theta = P_\theta / qh^2 = (\pi \cdot 10^5)/2 \approx 157079$ and $\widetilde{P}_s = P_s / qh^2 = 8\pi \times 10^4 \approx 251{,}327$. The convergence in three significant digits of the internal and external forces is achieved, as well as the convergence of the deflections $w_A$, at $K = 1281$ in the vertical section and at $K = 5121$ in the horizontal section. The convergence of the SSS components at the point $B$ $(w_B, \sigma^+, \sigma^-)$ is even slower and achieved at $K > 20481$.

Application of the mixed functional $\Pi_2(u, w, \varphi_s, T_{s\gamma}^f, \varepsilon_s^f)$ (6), in which the meridional strain $\varepsilon_s^f$ is additionally varied, made it possible to somewhat increase the convergence (Table 3) and to decrease the number of nodal points to 5121. Satisfactory accuracy of integral quantities and some SSS components is achieved at $K = 641$, and the signs of the deflection and moments at the point $B$ are valid (unlike Table 2) even at $K = 161$.

TABLE 3

| $K$ | $w_A$ | $w_B$ | $\sigma^+$, MPa | $\sigma^-$, MPa | $\widetilde{F}_\theta \cdot 10^{-5}$ | $\widetilde{F}_s \cdot 10^{-4}$ |
|---|---|---|---|---|---|---|
| 161 | 0.722 | 0.112 | –140 | 167 | 1.6003 | 24.0319 |
| 321 | 0.723 | 0.131 | –245 | 288 | 1.5825 | 33.5446 |
| 641 | 0.723 | 0.200 | –215 | 254 | 1.5764 | 25.1566 |
| 1281 | 0.723 | 0.218 | –199 | 237 | 1.5737 | 25.1415 |
| 2561 | 0.723 | 0.224 | –191 | 228 | 1.5723 | 25.1327 |
| 5121 | 0.723 | 0.227 | –186 | 223 | 1.5715 | 25.1327 |

**Conclusions.** The improvement of convergence due to the additional variation of the membrane strain is insignificant compared with other more demonstrative examples [10] can be attributed to the complex behavior of the SSS of a strongly extended toroidal shell that undergoes large bending in some parts and tension in other parts. Additional variation in the strain $\kappa_s^f$, i.e., change in the cross-sectional curvature of the shell, slightly improves the convergence compared with the variation of $\varepsilon_s^f$. The variation of the hoop strain components has appeared ineffective. Obviously, to decrease the moments, it is necessary to use shells of variable thickness [7, 17]. Thus, it may be concluded that the above problem can supplement the collection of so-called pathological tests for membrane locking.

## REFERENCES


1. A. N. Guz, A. S. Kosmodamianskii, V. P. Shevchenko, et. al., *Stress Concentration*, Vol. 7 of the twelve-volume series *Composite Mechanics* [in Russian], A.S.K., Kyiv (1998).
2. Yu. Yu. Abrosov, V. A. Maximyuk, and I. S. Chernyshenko, “Influence of cross-sectional ellipticity on the deformation of a long cylindrical shell,” *Int. Appl. Mech.*, **52**, No. 5, 529–534 (2016).
3. P. A. Bakusov and A. A. Semenov, “Stability of toroidal shell segments at variation of a deflection angle,” *PNRPU Mechanics Bulletin*, No. 3, 17–36 (2017).
4. I. S. Chernyshenko and V. A. Maximyuk, “On the stress-strain state of toroidal shells of elliptical cross-section formed from nonlinear elastic orthotropic materials,” *Int. Appl. Mech.*, **36**, No. 1, 90–97 (2000).
5. C. P. Fowler, A. C. Orifici, and C. H. Wang, “A review of toroidal composite pressure vessel optimization and damage tolerant design for high pressure gaseous fuel storage,” *Int. J. Hydrogen Energy*, **41**, No. 47, 22067–22089 (2016).
6. Y. Kisioglu, “Burst pressure determination of vehicle toroidal oval cross-section LPG fuel tanks,” *J. Pressure Vessel Technol.*, **133**, No. 3, 031202-1–031202-5 (2011).
7. I. V. Lutskaya, V. A. Maximuk, E. A. Storozhuk, and I. S. Chernyshenko, “Nonlinear elastic deformation of thin composite shells of discretely variable thickness,” *Int. Appl. Mech.*, **52**, No. 6, 616–623 (2016).
8. V. A. Maximyuk and I. S. Chernyshenko, “Nonlinear elastic state of thin-walled toroidal shells made of orthotropic composites,” *Int. Appl. Mech.*, **35**, No.12, 1238–1245 (1999).
9. V. A. Maximyuk, “Study of the nonlinearly elastic state of an orthotropic cylindrical shell with a hole using mixed functionals,” *Int. Appl. Mech.*, **37**, No. 12, 1602–1606 (2001).
10. V. F. Maximyuk, E. A. Storozhuk, and I. S. Chernyshenko, “Variational finite-difference methods in linear and nonlinear problems of the deformation of metallic and composite shells (review),” *Int. Appl. Mech.*, **48**, No. 6, 613–687 (2012).

11. M. D. Pazhooh, M. A. Dokainish, and S. Ziada, “Finite element modal analysis of on inflatable, self-rigidizing toroidal satellite component,” *Exper. Appl. Mech.*, **6**, No. 1, 281–288 (2011).
12. S. Roychowdhury and A. DasGupta, “Inflating a flat toroidal membrane,” *Int. J. Solids Struct.*, 67–68, 182–191 (2015).
13. E. J. Ruggiero, A. Jha, G. Park, and D. J. Inman, “A literature review of ultra-light and inflated toroidal satellite components,” *The Shock and Vibration Digest*, **35**, No. 3, 171–181 (2003).
14. E. A. Storozhuk and A. V. Yatsura, “Exact solutions of boundary-value problems for noncircular cylindrical shells,” *Int. Appl. Mech.*, **52**, No. 4, 386–397 (2016).
15. E. A. Storozhuk and A. V. Yatsura, “Analytical-numerical solution of static problems for noncircular cylindrical shells,” *Int. Appl. Mech.*, **53**, No. 3, 313–325 (2017).
16. W. J. Sutcliffe, “Stress analysis of toroidal shells of elliptical cross-section,” *Int. J. Mech. Sci.*, **13**, No. 11, 951–958 (1971).
17. V. T. Vu, “Minimum weight design for toroidal shells with strengthening component,” *J. Pressure Vessel Technol.*, **138**, No. 2, 21202-1–021202-7 (2015).
18. A. C. Young, W. G. Davids, D. J. Whitney, J. D. Clapp, and A. G. Goupee, “Structural testing and analysis of a braided, inflatable fabric torus structure,” *Acta Astronaut.*, **139**, 189–200 (2017).
19. A. Zingoni, N. Enoma, and N. Govender, “Equatorial bending of an elliptic toroidal shell,” *Thin-Walled Struct.*, **96**, 286–294 (2015).
20. L. Zu, S. Koussios, and A. Beukers, “A novel design solution for improving the performance of composite toroidal hydrogen storage tanks,” *Int. J. Hydrogen Energy*, **37**, No. 19, 14343–14350 (2012).